21. The Green Bank Ammonia Survey: Dense Cores Under Pressure in Orion A Kirk+ ApJ in press

GAS

$$\alpha = \frac{5\sigma_{tot}^2 R}{GM},$$

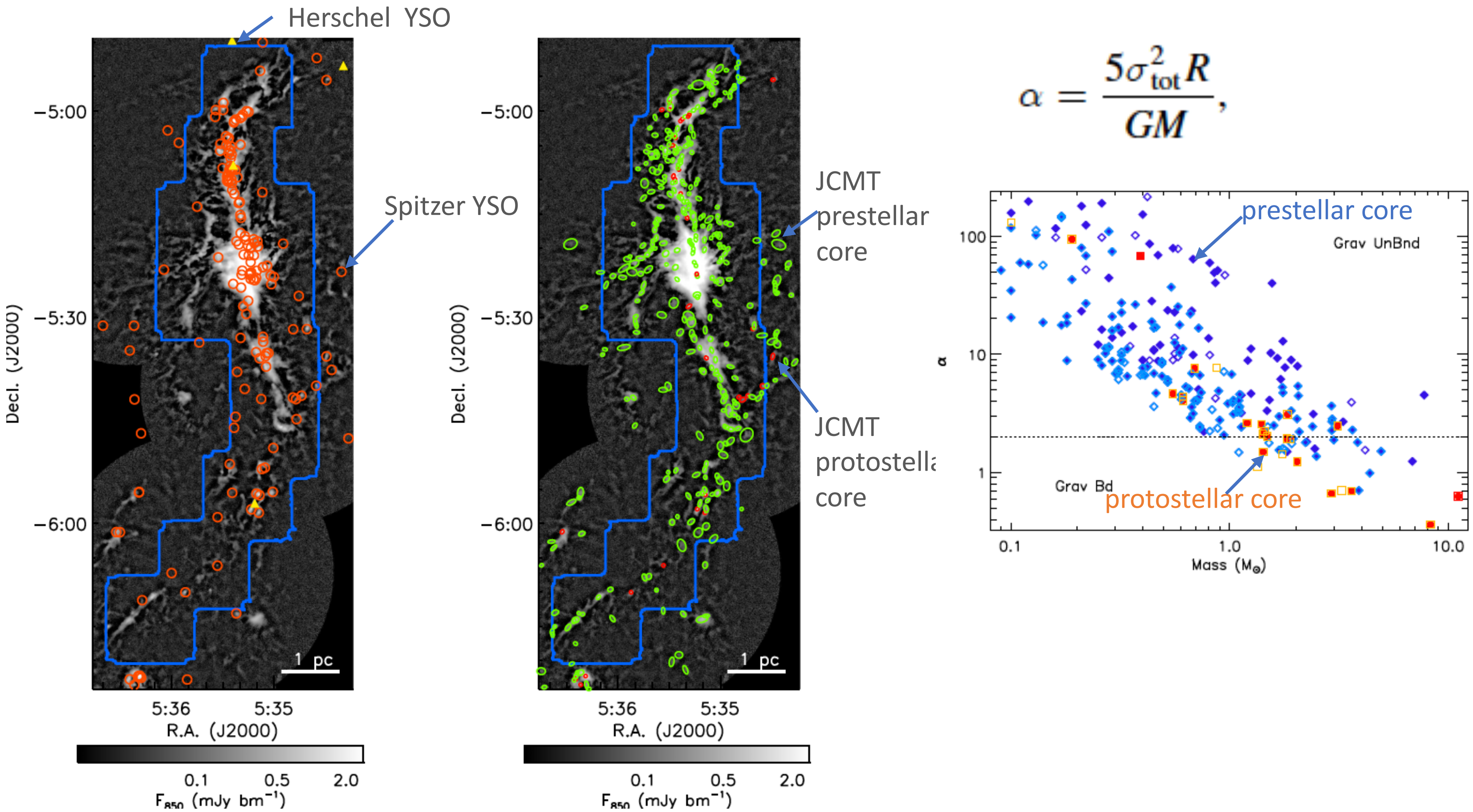

surface pressure $\Omega_P = -4\pi P R^3,$

potential $\Omega_G = \frac{-1}{2\sqrt{\pi}} \frac{GM^2}{R},$

kinetic energy $\Omega_K = \frac{3}{2} M \sigma_{\rm tot}^2,$

$-(\Omega_G+\Omega_P) = 2\Omega_K$

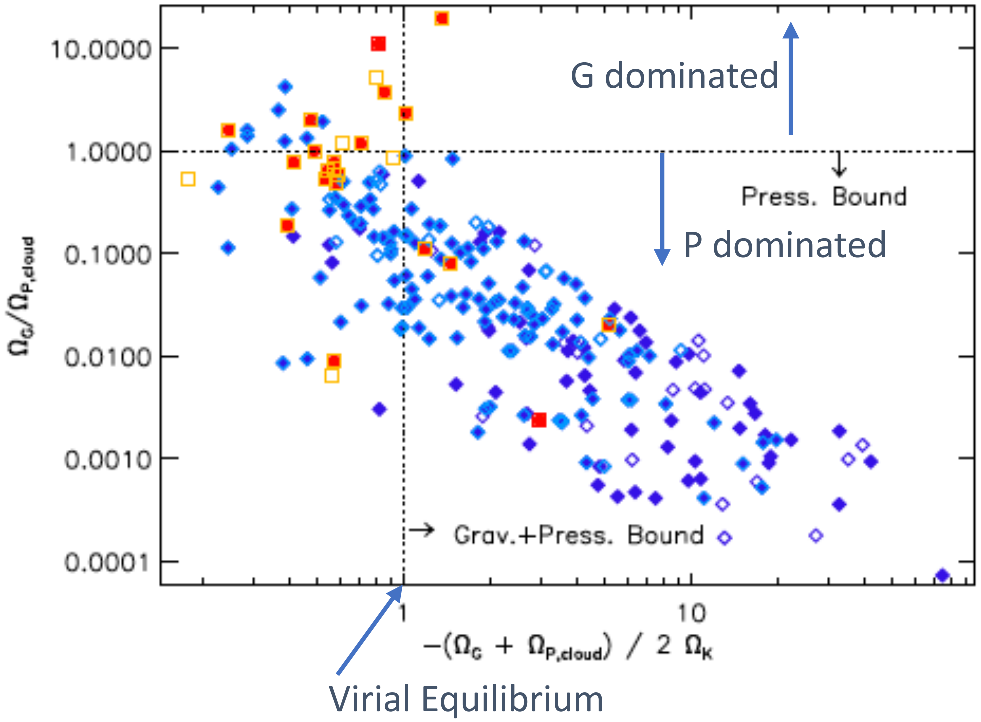

Surprisingly, we find that almost none of the dense cores are sufficiently massive to be bound when considering only the balance between self-gravity and the thermal and non-thermal motions present in the dense gas. Including the additional pressure binding imposed by the weight of the ambient molecular cloud material and additional smaller pressure terms, however, suggests that most of the dense cores are pressure-confined.

22. HP2 survey: III The California Molecular Cloud– A Sleeping Giant Revisited by Lada, Lewis, Lombardi, Alves Aap in press

SFR = 1/10 of Ori

Herschel data SED fit → (T, τ_{850})

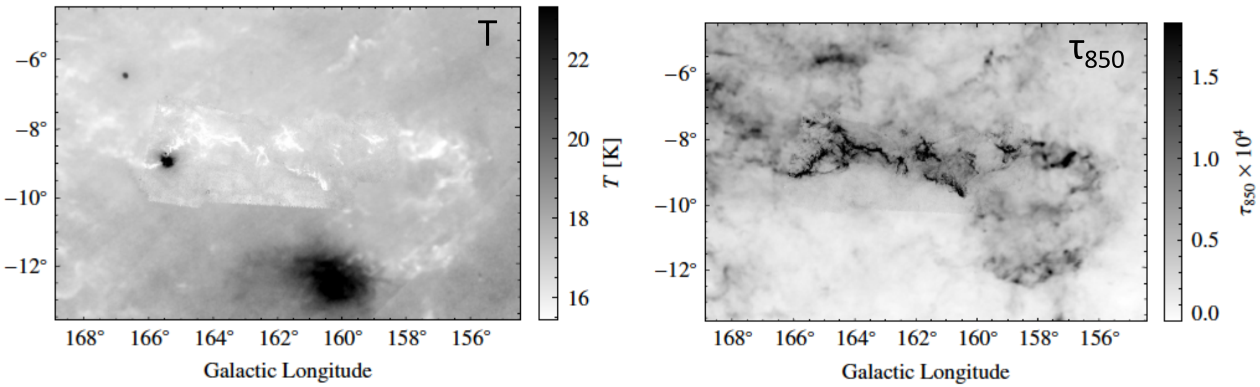

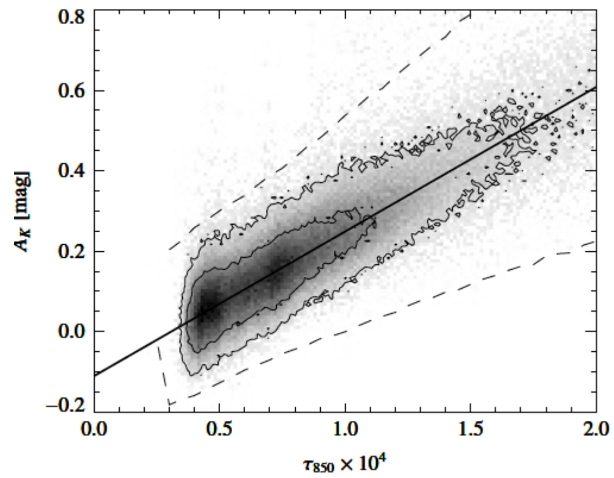

$$I_\nu = B_\nu(T)[1 - e^{-\tau_\nu}] \simeq B_\nu(T)\tau_\nu \,, \qquad \tau_\nu = \tau_{\nu_0}\left(\frac{\nu}{\nu_0}\right)^{\beta_d} \,,$$

$A_K = \gamma\tau_{850} + \delta$

γ=3593.75 mag

δ=-0.110 ± 0.006 mag

Structure Function

$$S(> A_K) \equiv \int_{A_K}^{\infty} \mathrm{d}S(A_K) \qquad \propto A_K^{-q}$$

where dS (A_K) is an element of cloud surface area at an extinction A_K.

derivative of this function

$dS(>A_K)/dAK = S'(>A_K) \propto A_K^{-n}$

proportional to the column density PDF

➔n=4.0 ± 0.1

➔q=3.0 (q=2 Ori A, B and Per)

➔steeper slope than the GMCs

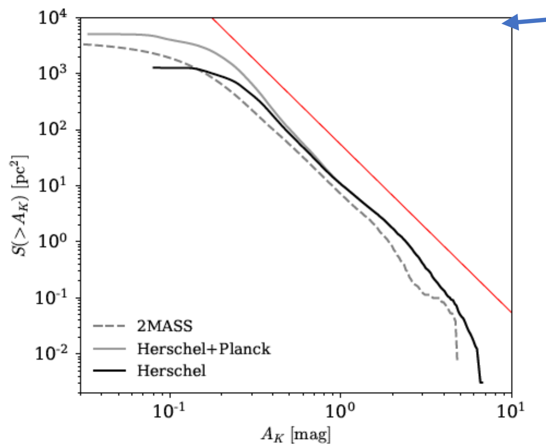

Fig. 8. The surface area distribution functions, $S(> A_K)$, for the California cloud. The solid red line represents a power law relation with a slope of −3 for comparison.

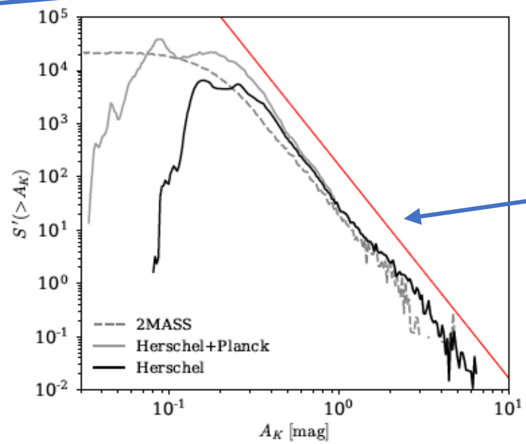

Fig. 9. The differential area function $-S'(> A_K)$ which is proportional to the probability density distribution for column densities in the cloud. In this plot a lognormal distribution would appear as a gaussian function whilst a power-law function would be a straight line. The red line shows the power-law $-S'(> A_K) \propto A_K^{-4.0}$. See text.

Schmidt Law

protostellar surface density: thresholded Schmidt relation

$$\Sigma_*(A_K) = \kappa\, A_K^{\beta}\, \mathrm{H}(A_K - A_{K,0}),$$

➔ $\beta=3.31 \pm 0.23$, $\kappa=0.36 \pm 0.09$ stars pc^{-2} $mag^{-3.31}$, $A_{K,0}=0.51$ mag.

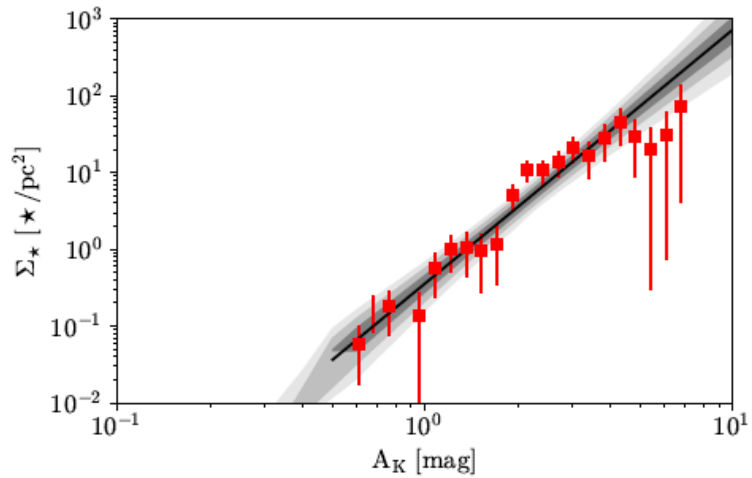

Table 1. Schmidt relation and PDF power-law indicies for GMCs studied with *Herschel*

GMC	β	Reference	n	Reference
California	3.31 ± 0.23	1	4.0	1
Orion A	1.99 ± 0.05	2	2.9	4
Orion B	2.16 ± 0.10	2	3.0	4
Perseus	2.4 ± 0.6	3	2.7	4

References. (1) This paper; (2) Lombardi et al. (2014); (3) Zari et al. (2016) (4) Lombardi et al. (2015).

unknown $\mathrm{PDF}_*(A_K) \equiv \frac{1}{N_{*tot}} \frac{dN_*(A_K)}{dA_K}$

measured

measured

$$\Sigma_*(A_K) = \frac{\mathrm{d}N_*(A_K)}{\mathrm{d}S(A_K)} = \Sigma_{*0} \times \frac{\mathrm{PDF}_*(A_K)}{\mathrm{PDF}_N(A_K)}$$

$$\mathrm{PDF}_*(A_K) = \frac{\Sigma_*(A_K)}{\Sigma_{*0}} \times \mathrm{PDF}_N(A_K)$$

if power law → $p=\beta-n = -0.69 \pm 0.27$

$\propto A_k^p$

$$N_*(>A_K)/N_{*tot} = \int_{A_K}^{\infty} \mathrm{PDF}_*(A_K)\mathrm{d}A_K$$

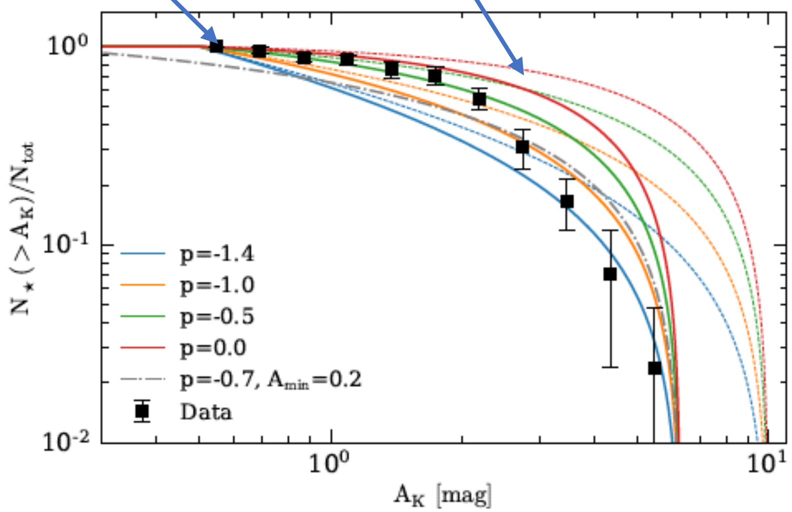

Our observations suggest that variations both in the slope of the Schmidt relation and in the sizes of the protostellar populations between GMCs are largely driven by variations in the slope, n, of $\mathrm{PDF}_N(A_K)$.

23. Mid-Infrared Polarization of Herbig Ae/Be Discs by Dan Li+, MNRAS in press

The translation of mm/submm polarization maps into the B-field morphology (projected on the plane-of-sky) was once thought to be straightforward, but recent studies have emphasized that scattered emission can also contribute to the observed mm/submm polarization if dust grains much larger than their ISM (interstellar medium) counterparts are present in discs (Kataoka et al. 2015; Yang et al. 2016; Tazaki et al. 2017).

(1) Observation: a mid-infrared (mid-IR) polarimetry using Canari-Cam
(2) Object: Herbig Ae/Be (HAeBe) stars (i.e., premain sequence stars of 2–8 $M_\odot$).
(3) detected: the brightest and most compact inner regions of the discs.
(4) Band: Si-2 (λ=8.7μm), Si-4 (λ=10.3μm), Si-6 (λ=12.5μm)

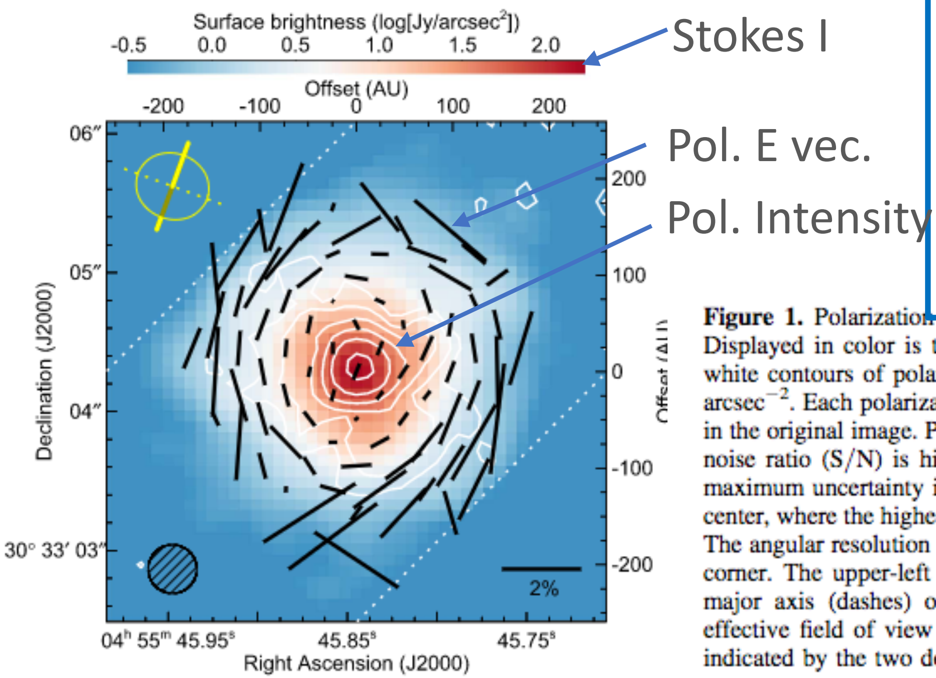

AB Aur (Li+ 2016)
r>70AU ring-like (scattering),
r<70AU PA~165deg (dichroic emission of elongated particles aligned in a disk *B*-field [poloidal axis is offset from disk axis])

Figure 1. Polarization map of the AB Aur protoplanetary disk at 10.3 μm. Displayed in color is the total intensity image of the disk, superimposed by white contours of polarized intensities at 20, 40, 80, 160, 320, and 640 mJy arcsec^{-2}. Each polarization vector is derived from an aperture of 3 × 3 pixels in the original image. Polarization vectors are only plotted where the signal-to-noise ratio (S/N) is higher than 150 in the total intensity image, yielding a maximum uncertainty in the degree of polarization (p) of ~1%. Near the disk center, where the highest S/N is reached, the typical uncertainty in p is ~0.1%. The angular resolution of the observation is 0.″35, as shown in the bottom-left corner. The upper-left sketch shows the projected spin axis (thick line) and major axis (dashes) of the disk. In the dual-beam polarimeter mode, the effective field of view of CanariCam is a long rectangle ~2.″7 in height, as indicated by the two dotted lines.

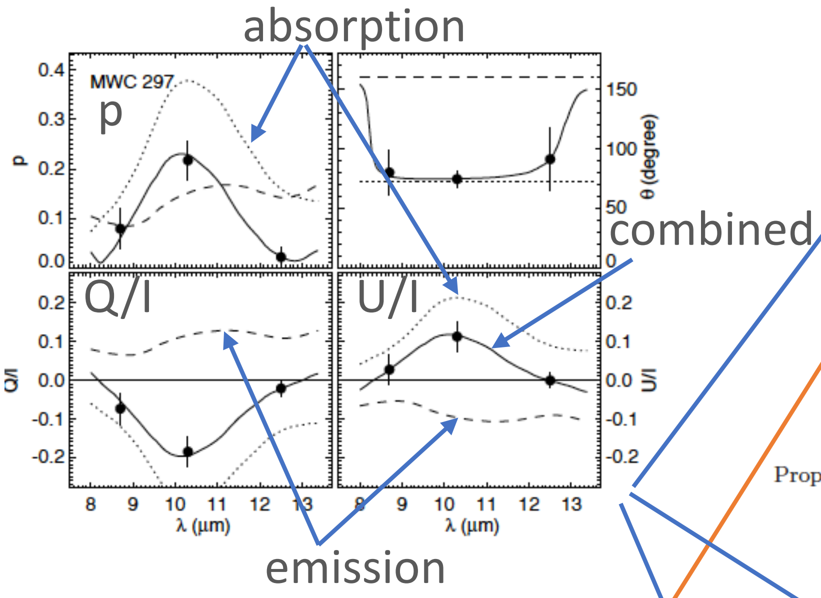

Object	λ (µm)	F_ν (Jy)	p (per cent)	θ (degree)
MWC 297	8.7	115.9 ± 11.6	0.08 ± 0.05	80 ± 19
	10.3	103.2 ± 10.3	0.22 ± 0.05	74 ± 7
	12.5	111.6 ±11.2	0.02 ± 0.03	91 ± 26
HD 200775	8.7	7.8 ± 0.8	0.47 ± 0.09	105 ± 2
	10.3	7.3 ± 0.7	0.52 ± 0.15	110 ± 1
	12.5	5.3 ± 0.5	1.2 ± 0.1	111 ± 1

Properties of discs and interstellar B-fields.

Object	10-µm Silicate Feature Type	Disc P.A. (degree)	Inclination (degree)	Ref.	IS B-field P.A.[a] (degree)	Ref.
MWC 1080A	Abs	135 ± 5	55 ± 5	1,2	70	19
MWC 297	Abs	165 ± 15	13 ± 5	1,3	40	19,20
HD 200775	Em	6.9 ± 1.5	54.5 ± 1.2	1,4	142	19
VV Ser	Em	15 ± 5	72 ± 5	5	60	20,21
HD 179218	Em	22 ± 3	56 ± 2	1,9	4	20
AB Aur	Em	70 ± 10	27 ± 5	6–8	70	19,22
HD 163296	Em	136 ± 2	48 ± 2	10	175	23
MWC 480	Em	148 ± 2	38 ± 5	11–13	–	
MWC 758	Em	65 ± 7	21 ± 2	14	–	
CQ Tau	Em	54 ± 1	29 ± 2	15,16	42	24
HL Tau	Abs	138.02 ± 0.07	46.72 ± 0.05	17,18	77	25

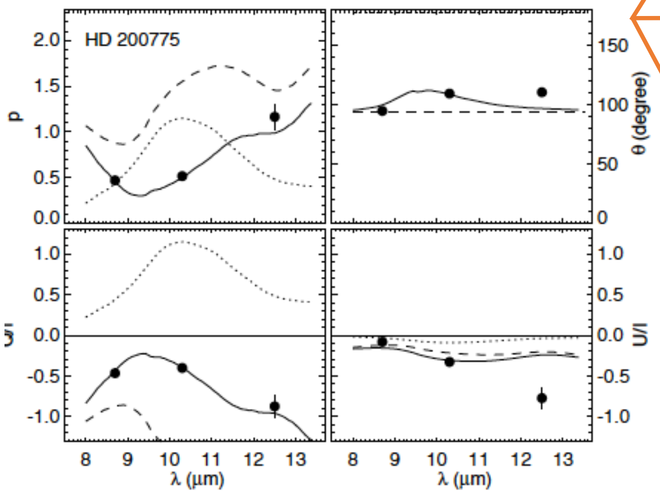

not inconsistent with
2 component model
→ scattering

Object	Scattering	Emission	Absorption	B-field
MWC 1080A			√	Complex or tilted
MWC 297		√	√	Poloidal[a]
HD 200775	√			
VV Ser	√	√	√	Toroidal
HD 179218	√	√		Toroidal
AB Aur	√	√		Tilted poloidal (L16)
HD 163296				
CQ Tau		√		Complex or tilted
HL Tau			√	Complex or tilted

Possible origin(s) of polarization. See Section 4.3 for details.
[a] Poorly constrained. See Section 4.3.

24. The Formation of Stellar Clusters in Magnetized, Filamentary Infrared Dark Clouds
Pak Shing Li et al. MNRAS in press

InfraRed Dark Cloud Σ~10^22cm^-2 ρ~10^4cm^-3 M~10^2~10^3 M_sol
λ >> 2c_s^2/G ~16.6 (T/10K) M_sol/pc

(1) Would stars form throughout the lament, or would the formation propagate along the lament?
(2) How efficient is protostellar feedback in destroying or disrupting a lament?
(3) Would the geometry of long filamentary clouds affect the properties of a protostellar cluster, such as the protostellar mass function (PMF) and the companion multiplicity?

Model and Method
Numerical Methods:orion2 adaptive mesh renement (AMR) code
Turbulence: M=10, M_A=1 driving turbulence, T=10K, M=3110M_sol, V=(4.55pc)^3
sink particle:
stellar feedback: Luminosity + outflow (momentum+energy)
fw=Mdot ej/Mdot acc=0.3; outflow speed v_w=min[v_Kep(R_*)/3, 100km/s]

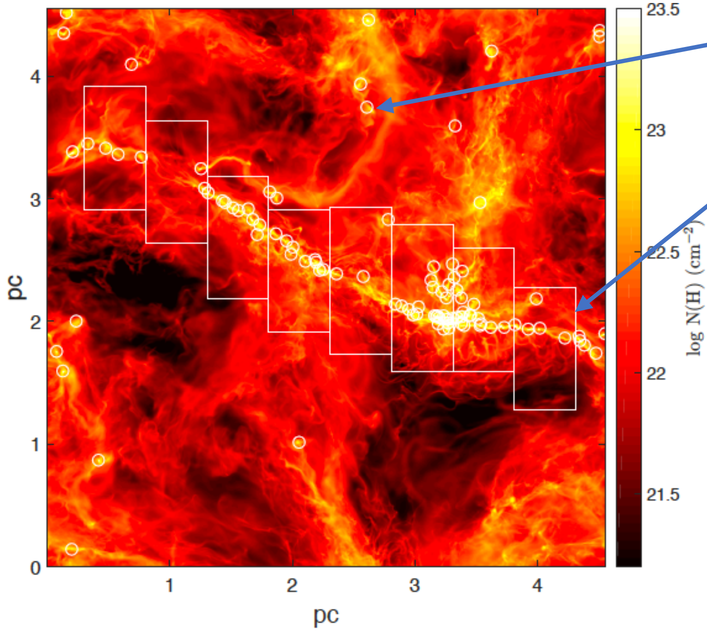

100 most massive clumps

zoom-in region=refine upto 6 levels

$$\epsilon_{\rm ff} \equiv \frac{\dot{M}_{*,\rm obs}}{M_g/t_{\rm ff}},$$

Krumholz+12 → high z gal 0.015

Heyer+16 → Class I 0.02

εff=0.067

Chabrier IMF05

Mass Func

M*tot= 5.0 M$_\odot$ — evolution → 28.6 M$_\odot$

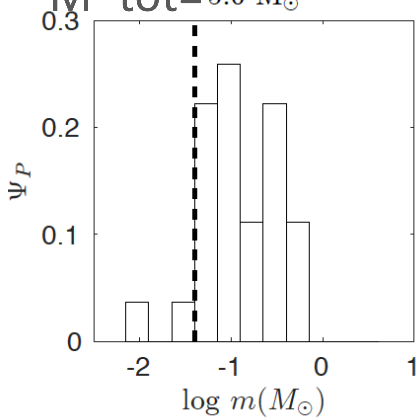

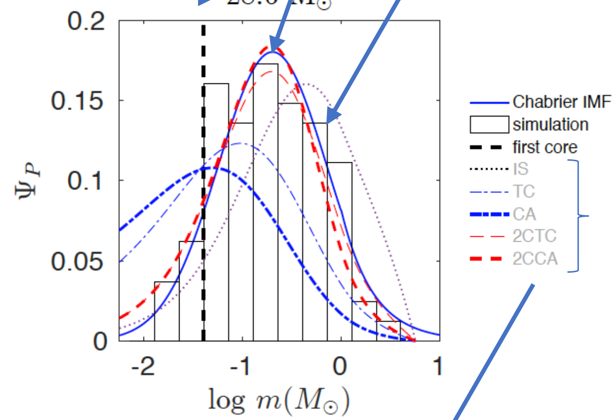

theoretical IMF

SFE=M*/(Mg+M*)

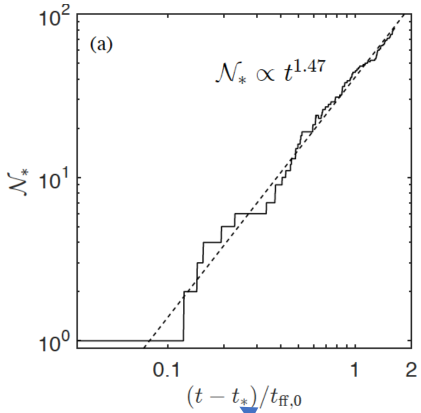

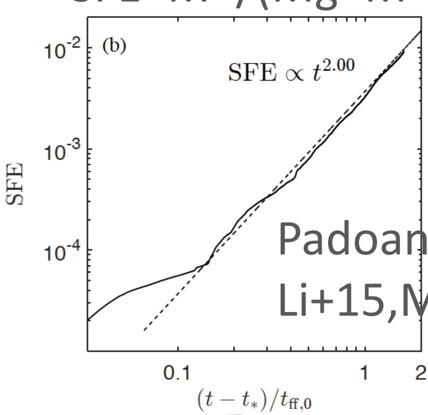

Padoan+14 →1.75

Li+15,Murray+17 →2

Luminosity Prob ➔ resolved

1st protostar is made

25. The properties of the inner disk around HL Tau: Multi-wavelength modeling of the dust emission by Yao Liu+ AAp in press

Carrasco-Gonzalez+2016
VLA 7mm cont.

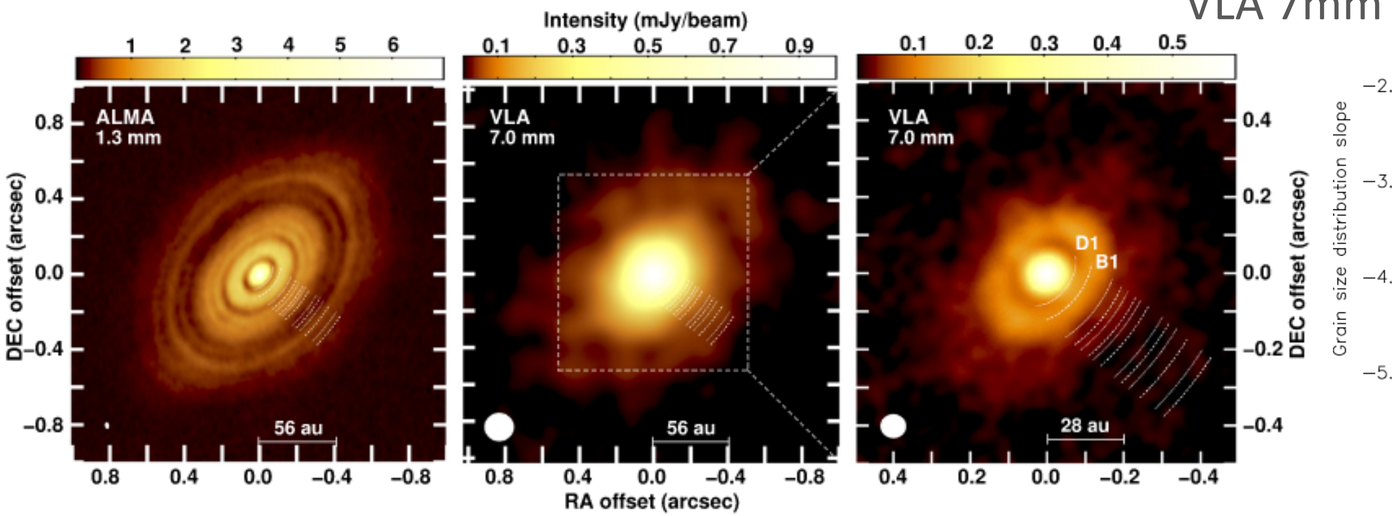

Figure 1. Comparison between the ALMA and VLA observations of the HL Tau disk. Left: ALMA image at 1.3 mm. Center: VLA image at 7.0 mm with an angular resolution of ~20 au (0.″15; tapered image). Right: close-up of the center of the disk. VLA image at 7.0 mm with an angular resolution of ~10 au (~0.″07; natural weighting). In all panels, the positions of the reported dark (D1–D7; dotted lines) and bright (B1–B7; dashed lines) rings from the ALMA images (ALMA Partnership et al. 2015a) are shown. The inner disk and the first pair of dark (D1) and bright (B1) rings are clearly seen in the 7.0 mm images.

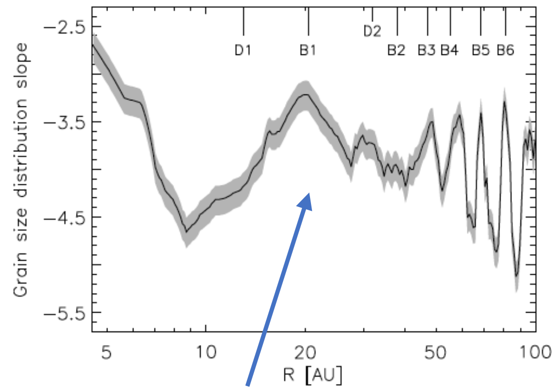

Fig.6: larger grains are trapped in the first bright ring.

ALMA wavelengths of 2.9, 1.3, and 0. 87mm revealed a pattern of bright and dark rings.

(1) embedded planets in the gaps (Dong+2015; Dipierro+ 2015; Picogna & Kley 2015)→ Large Binocular Telescope, however, excluded the presence of massive planets (~ 10 – 15MJup) in two gaps ~70AU (Testi+2016)

(2) non ideal MHD (Flock+2015)

(3) sintering（焼結）-induced dust rings (Okuzumi+ 2016),

(4) dust coagulation triggered by condensation zones of volatiles (Zhang et al. 2015),

(5) secular gravitational instability (Takahashi & Inutsuka 2016).

Since radiation λ=2.9mm optically thick, longer wavelength λ=7mm (JVLA)

Flared disk

$$\rho_{\rm dust} \propto \Sigma(R) \times \exp\left[-\frac{1}{2}\left(\frac{z}{h(R)}\right)^2\right],$$

→β>1

$$h(R) = H_{100}\left(\frac{R}{100\,\rm AU}\right)^{\beta},$$

ξ>0 smaller dust has a larger scaleheight

$$H_{100}(a) = H_{100}(a_{\rm min})\left(\frac{a}{a_{\rm min}}\right)^{-\xi}.$$

dust size distribution a=(0.01μm,7mm

$$dn(a) \propto a^p da$$

p=-3.5 or spatially varies

Central Star $M_*=1.7M_\odot$, T=4000K, $L=11L_\odot$

Disk parameters			
β	1.15	$1.14^{+0.018}_{-0.007}$	$1.08^{+0.03}_{-0.005}$
$H_{100}(a_{\rm min})$ [AU]	15	$13.7^{+1.6}_{-1.0}$	$10.6^{+4.3}_{-1.1}$
$M_{\rm dust}$ [$10^{-3}\,M_\odot$]	1.0	$1.0^{+0.12}_{-0.1}$	$1.0^{+0.07}_{-0.16}$
p	−3.5	–	–
$p_{\rm inner}$	–	$-3.45^{+0.08}_{-0.17}$	–
$p_{\rm outer}$	–	$-3.92^{+0.18}_{-0.08}$	–
$f_{\rm inner}$	–	$0.5^{+0.03}_{-0.11}$	–
$f_{2.82}$	–	–	$0.27^{+0.05}_{-0.07}$
$f_{0.95}$	–	–	$0.15^{+0.07}_{-0.03}$
$f_{0.45}$	–	–	$0.20^{+0.03}_{-0.06}$
$f_{0.29}$	–	–	$0.15^{+0.05}_{-0.05}$
Observational parameters			
i [°]		46.7	
Position angle [°]		138	
D [pc]		140	

Notes. (1) Model A is used in the derivation of the surface density profile (see Sect. 3). (2) Model B and C correspond to the best-fit models under an assumption of two power-law grain size distributions (see Sect. 5.2) and a complex grain size distribution (see Sect. 5.3), respectively.

(A) Modeling with a homogeneous grain size distribution →NO

(B) Modeling with two power-law grain size distributions

cf. Pinte+2016 model p=-3.5 @ r<75AU; -4.5 @ r>75AU

$p_{\rm inner} = -3.5^{+0.1}_{-0.2}$ @ r<50AU; $p_{\rm outer} = -3.9^{+0.2}_{-0.1}$ @ r>50AU

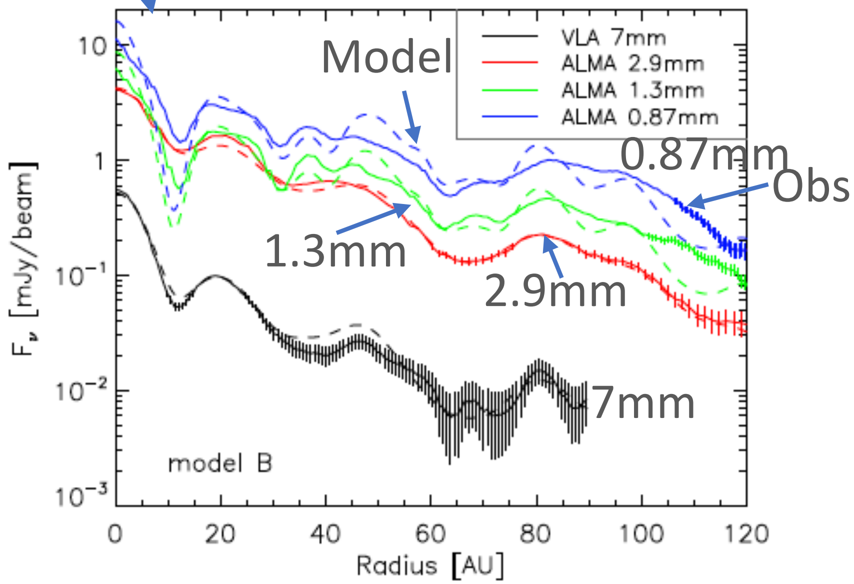

(C) mass fraction $f_{\rm size}$ @ size= 2.82, 0.95, 0.45, and 0.29mm

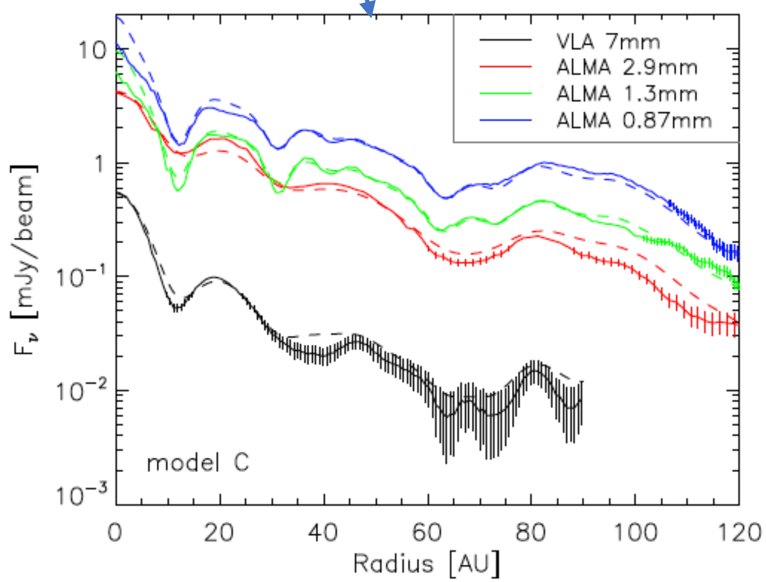

$$\Sigma(r) \propto r^{-q}$$

$$h(r) = h_0(r/r_0)^{\gamma},$$

$$n(a) \propto a^{-3.5}$$

Model Parameters

Parameter	Value	Unit
T_*	10,000	K
R_*	2.5	$R_\odot$
Inclination	27	Degree
r_{in}	0.5	au
r_{out}	400	au
q	1.2	...
r_0	100	au
h_0	8.5	au
γ	1.125	...
M_{dust}	1.2e-4	$M_\odot$
a_{min}	0.01	μm
a_{max}	1.0	μm

Note. Emission of the star is assumed to be blackbody.

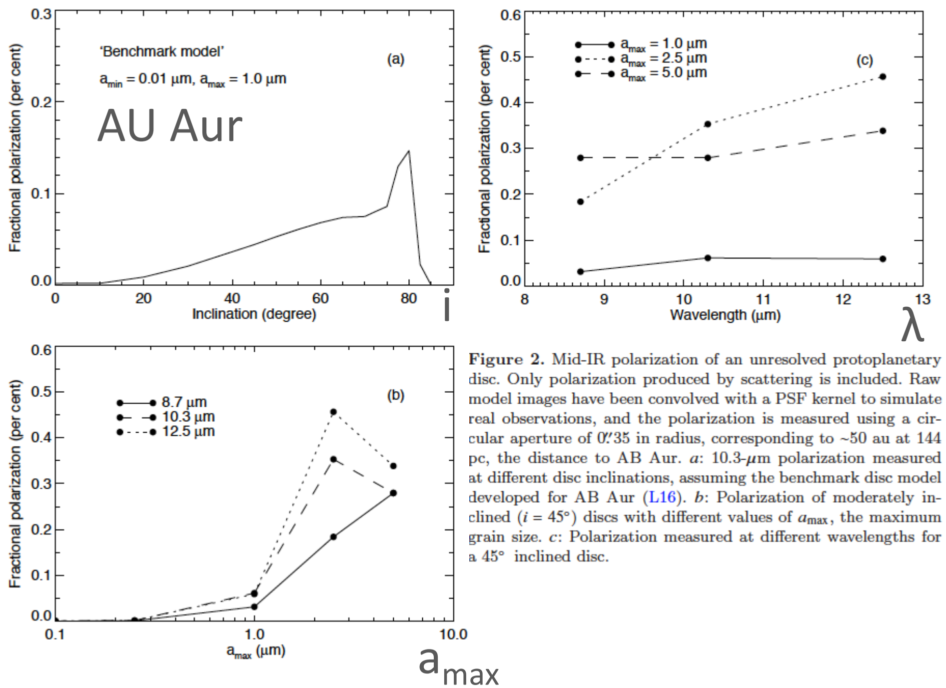

Figure 2. Mid-IR polarization of an unresolved protoplanetary disc. Only polarization produced by scattering is included. Raw model images have been convolved with a PSF kernel to simulate real observations, and the polarization is measured using a circular aperture of 0.″35 in radius, corresponding to ~50 au at 144 pc, the distance to AB Aur. *a*: 10.3-μm polarization measured at different disc inclinations, assuming the benchmark disc model developed for AB Aur (L16). *b*: Polarization of moderately inclined (i = 45°) discs with different values of $a_{\max}$, the maximum grain size. *c*: Polarization measured at different wavelengths for a 45° inclined disc.